

REPORT DOCUMENTATION PAGE				Form Approved OMB No. 0704-0188	
Public reporting burden for this collection of information is estimated to average 1 hour per response, including the time for reviewing instructions, searching existing data sources, gathering and maintaining the data needed, and completing and reviewing this collection of information. Send comments regarding this burden estimate or any other aspect of this collection of information, including suggestions for reducing this burden to Department of Defense, Washington Headquarters Services, Directorate for Information Operations and Reports (0704-0188), 1215 Jefferson Davis Highway, Suite 1204, Arlington, VA 22202-4302. Respondents should be aware that notwithstanding any other provision of law, no person shall be subject to any penalty for failing to comply with a collection of information if it does not display a currently valid OMB control number. PLEASE DO NOT RETURN YOUR FORM TO THE ABOVE ADDRESS.					
1. REPORT DATE (DD-MM-YYYY) 25-01-2007		2. REPORT TYPE Journal Article		3. DATES COVERED (From - To)	
4. TITLE AND SUBTITLE  Ultrahydrophobic Fluorinated Polyhedral Oligomeric Silsesquioxanes (F-POSS) (Preprint)				5a. CONTRACT NUMBER	
				5b. GRANT NUMBER	
				5c. PROGRAM ELEMENT NUMBER	
6. AUTHOR(S) Joseph M. Mabry, Scott T. Iacono, & Brent D. Viers (AFRL/PRSM); Ashwani Vij (AFRL/PRSP)				5d. PROJECT NUMBER 23030521	
				5e. TASK NUMBER	
				5f. WORK UNIT NUMBER	
7. PERFORMING ORGANIZATION NAME(S) AND ADDRESS(ES)  Air Force Research Laboratory (AFMC) AFRL/PRSM 9 Antares Road Edwards AFB CA 93524-7401				8. PERFORMING ORGANIZATION REPORT NUMBER  AFRL-PR-ED-JA-2007-055	
9. SPONSORING / MONITORING AGENCY NAME(S) AND ADDRESS(ES)  Air Force Research Laboratory (AFMC) AFRL/PRS 5 Pollux Drive Edwards AFB CA 93524-7048				10. SPONSOR/MONITOR'S ACRONYM(S)	
				11. SPONSOR/MONITOR'S NUMBER(S) AFRL-PR-ED-JA-2007-055	
12. DISTRIBUTION / AVAILABILITY STATEMENT  Approved for public release; distribution unlimited (PA #07028A)					
13. SUPPLEMENTARY NOTES To be published in Angewante Chemie.					
14. ABSTRACT  Recently, significant attention has been drawn to preparing low surface energy materials inspired by naturally evolved biological systems possessing a high degree of ultrahydrophobicity. <sup>[1]</sup> Specifically, the lotus leaf exhibits an inherent self-cleaning mechanism resulting from micron-sized waxy nodes protruding from its surface so that water is naturally repelled removing any foreign debris. <sup>[2,3]</sup> This remarkable cleansing mechanism, coined the "lotus effect," has been artificially mimicked to produce materials with pronounced ultrahydrophobicity. Notable examples include surface patterning, <sup>[4]</sup> molecular self-assembly, <sup>[5]</sup> deposition <sup>[6]</sup> , and etching. <sup>[7]</sup> However, these examples require aggressive chemical surface treatments, high temperature post-surface modification, elaborate patterning, or necessitate the need for limitedly accessible deposition equipment. For such reasons, there exists a demand to construct ultrahydrophobic materials inspired by nature that are easy to prepare on a large scale.					
15. SUBJECT TERMS					
16. SECURITY CLASSIFICATION OF:			17. LIMITATION OF ABSTRACT  SAR	18. NUMBER OF PAGES  11	19a. NAME OF RESPONSIBLE PERSON Dr. Joseph M. Mabry
a. REPORT Unclassified	b. ABSTRACT Unclassified	c. THIS PAGE Unclassified			19b. TELEPHONE NUMBER (include area code) N/A

# Ultrahydrophobic Fluorinated Polyhedral Oligomeric Silsesquioxanes (F-POSS)

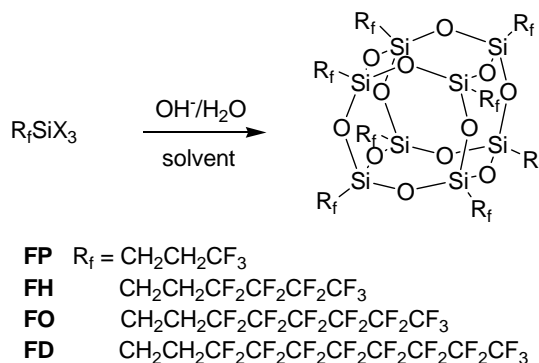
Joseph M. Mabry,\* Ashwani Vij,\* Scott T. Iacono, and Brent D. Viers

Recently, significant attention has been drawn to preparing low surface energy materials inspired by naturally evolved biological systems possessing a high degree of ultrahydrophobicity.<sup>[1]</sup> Specifically, the lotus leaf exhibits an inherent self-cleaning mechanism resulting from micron-sized waxy nodes protruding from its surface so that water is naturally repelled removing any foreign debris.<sup>[2,3]</sup> This remarkable cleansing mechanism, coined the "lotus effect," has been artificially mimicked to produce materials with pronounced ultrahydrophobicity. Notable examples include surface patterning,<sup>[4]</sup> molecular self-assembly,<sup>[5]</sup> deposition<sup>[6]</sup>, and etching.<sup>[7]</sup> However, these examples require aggressive chemical surface treatments, high temperature post-surface modification, elaborate patterning, or necessitate the need for limitedly accessible deposition equipment. For such reasons, there exists a demand to construct ultrahydrophobic materials inspired by nature that are easy to prepare on a large scale.

Polyhedral oligomeric silsesquioxanes (POSS) are thermally robust cages consisting of a silicon-oxygen core framework possessing alkyl functionality on the periphery and are used for the development of high performance materials in medical, aerospace, and commercial applications.<sup>[8]</sup> Unlike other nano-fillers for high performance material enhancement (silica, clays, nanotubes, nanofibers), POSS molecules can be functionally tuned and are easily synthesized with inherent functionality, are discreetly nano-sized, and often commercially available. Furthermore, POSS possesses a high degree of compatibility in blended polymers and can also be easily covalently linked into a polymer backbone.<sup>[9]</sup> The incorporation of POSS into polymers produces hybrid composite properties improving, although not limited to, glass transition temperature, mechanical strength, thermal and chemical resistance, and ease of processing. In this work, we demonstrate the facile preparation of a novel class of fluorinated POSS (F-POSS) materials possessing ultrahydrophobicity as a result of low surface energy fluoroalkyl chains and their ability to induce both nanometer- and micron-scale roughness.

Fluorinated nanoparticles are of particular interest in the academic community. There have been many reported attempts to synthesize and characterize partially or fully fluorinated nanoparticles. These reports include the fluorination or fluoro-alkylation of C<sub>60</sub>.<sup>[11]</sup> X-ray analysis is complicated by the presence of both D<sub>3</sub> and S<sub>6</sub> isomeric C<sub>60</sub>F<sub>48</sub> molecules.<sup>[12]</sup> A perfluorocarborane, perfluoro-deca-*B*-methyl-*para*-carborane, has also been produced.<sup>[13]</sup> This compound is surprisingly stable to hydrolysis and oxidation. Crystal structures of this compound have also been obtained. Fluorinated carbon nanotubes and nanofibers have also been produced.<sup>[14]</sup> Characterization indicates that fluorine atoms may be present in both covalent and ionic forms.

F-POSS synthesis is shown in Scheme 1. This process is a base-catalyzed condensation of trialkoxysilanes in alcoholic media. The yields are nearly quantitative. Several compounds have been produced *via* this method, including (1H,1H,2H,2H-heptadecafluorodecyl)<sub>8</sub>Si<sub>8</sub>O<sub>12</sub> (**FD**), (1H,1H,2H,2H-tridecafluorooctyl)<sub>8</sub>Si<sub>8</sub>O<sub>12</sub> (**FO**), (1H,1H,2H,2H-nonadecafluorohexyl)<sub>8</sub>Si<sub>8</sub>O<sub>12</sub> (**FH**), and (3,3,3-trifluoropropyl)<sub>8</sub>Si<sub>8</sub>O<sub>12</sub> (**FP**) POSS. Once produced, these compounds are soluble in many fluorinated solvents. The exception is **FP**, which is soluble in common organic solvents. The melting points for these compounds are between 120 and 150 °C, with the exception of **FP**, which melts at approximately 235 °C. This high melting point is likely due to increased intimate intermolecular Si•••F contacts. Thermogravimetric (TGA) analysis indicates that these compounds volatilize, rather than decompose in both nitrogen and air. **FD** is the most stable, subliming at approximately 325 °C in nitrogen and 300 °C in air. F-POSS are also very dense, high molecular weight materials. For example, **FD** has a molecular weight of 3993.54 g/mol and a density of 2.067 g/mL.



**Scheme 1.** Base-catalyzed condensation of F-POSS compounds **FP**, **FH**, **FO**, and **FD**.

[\*] Dr. J. M. Mabry,\* Dr. A. Vij,\* S. T. Iacono, Dr. B. D. Viers  
Space and Missile Propulsion Division  
Air Force Research Laboratory  
10 E. Saturn Blvd., Edwards AFB, CA 93524 (USA)  
Fax: (+1) 661-275-5857  
E-mail: joseph.mabry@edwards.af.mil

[\*\*] The authors would like to thank the Air Force Office of Scientific Research and the Air Force Research Laboratory, Propulsion Directorate for their support. We would also like to thank Ms. Sherly Largo for her assistance with AFM images and Dr. Timothy Haddad for his technical support.



Supporting information for this article is available on the WWW under <http://www.angewandte.org> or from the author.

The hydrophobicity of spin-cast F-POSS surfaces was tested using water drop shape analysis and measured for the corresponding water contact angle (Figure 1). The relationship of contact angle and surface energy is governed by the Young's equation, which relates interfacial tension of the surface to the liquid and gas phases of water.<sup>[14]</sup> Although the trend shows that the F-POSS water contact angles increase with increasing fluorocarbon chain length, it does not explain the significant increase in contact angle from **FO** to **FD**. F-POSS were found to be surprisingly hydrophobic. **FD** is actually ultrahydrophobic, with a water contact angle over 150°. In fact, **FO** and **FD** are so hydrophobic that, even with a density over 2 g/mL, crystals of these F-POSS compounds float on the surface of water.

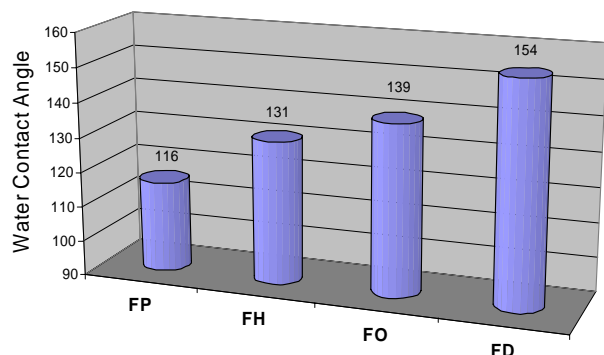


**Figure 1.** Graph showing water contact angles of **FP**, **FH**, **FO**, and **FD**. The hydrophobicity increases with the fluoroalkyl chain length.

It is well known that hydrophobicity is a function of both surface tension and surface roughness, as demonstrated by Cassie and Wenzel.<sup>[15,16]</sup> Figure 2 (a) is a height image taken with an atomic force microscope (AFM) of a spin-cast **FD** surface. This surface has a root mean squared (rms) roughness value of approximately four microns. Surfaces of all F-POSS compounds were prepared in the same way, with similar surface roughness in microns. Figure 2 (b) is an image of a drop of water on the same surface shown in Figure 2 (a). The contact angle at the interface was measured manually and *via* software at 154°.

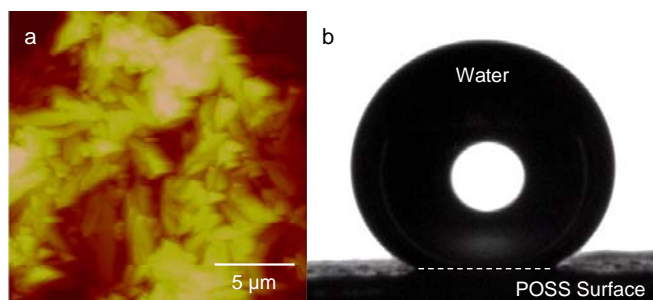


**Figure 2.** (a) Atomic Force Microscopy height image of spin-cast **FD** surface and (b) image of water drop on same surface with contact angle of 154°.

Crystals of F-POSS samples have been grown by solvent evaporation and single crystal X-ray structures have been obtained. **FH** and **FD** are shown at the top of Figure 3. From these structures, it can be observed that the electropositive silicon atoms interact with electron rich fluorine atoms. These interactions can be both intramolecular or intermolecular in nature with Si...F interaction at distances less than the sum of van der Waal radii for silicon and fluorine (2.10 and 1.47 Å, respectively).<sup>[17]</sup>

A trend was observed between the crystal structures of the F-POSS compounds in conjunction with the water contact angles. **FP** has a modest hydrophobicity due to short fluorocarbon chain length. **FH** and **FO** have similar water contact angles, as well as similar structures, as observed by X-ray analysis. Both appear to have a flat surface on one side. **FD**, on the other hand, exhibits a much higher contact angle. The structure of **FD** also appears to be significantly different. The structure of **FD** is bent at the methylene groups adjacent to the silicon atoms. This bent structure leads to a nano-

scale molecular surface roughness that contributes to ultrahydrophobicity. Nanoroughness has been shown to experimentally and theoretically increase hydrophobicity of a surface, albeit the changes in water contact angle are noticeably modest.<sup>[18]</sup> Shown at the bottom of Figure 3 are computer generated surfaces of **FH** and **FD** using the actual X-ray crystal structures. One can see that the **FH** surface, similar to the **FO** surface, can be grown in such a manner that there is a relatively flat surface. The **FD** surface is very different. Because of the bent structure, a flat crystal surface cannot be obtained. It is this nano-scale difference in the surface roughness, in combination with the micro-scale spin-casting roughness, which produces the ultrahydrophobicity of the **FD** surface.

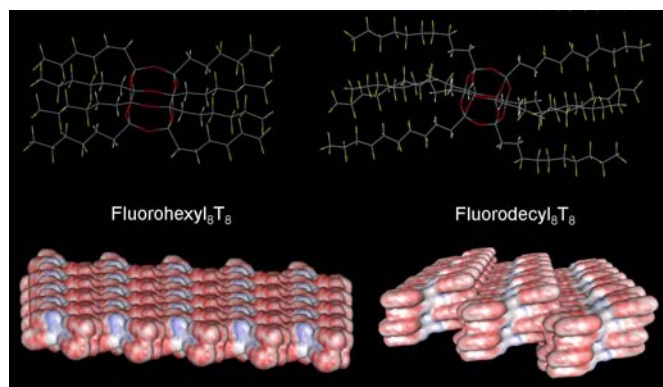


**Figure 3.** Crystal structures of **FH** and **FD** (top) and electrostatic potential surfaces for crystals of **FH** and **FD**, where **FD** exhibits nano-scale surface roughness, while **FH** does not. (bottom).

Hydrophobicity of **FD** was compared to a commercial grade of poly(tetrafluoroethylene) (PTFE). As shown in Figure 4, the **FD** water contact angle was 40% higher than PTFE, which was measured at 110°. As an extension of surface energy analysis, other test fluids such as a polar hydrocarbon (CH<sub>2</sub>I<sub>2</sub>) and nonpolar hydrocarbon (*n*-decane) were also measured to determine oleophobicity. The **FD** solid surface showed 55% and 143% higher hydrocarbon contact angle compared to PTFE for CH<sub>2</sub>I<sub>2</sub> and *n*-decane, respectively. These results show the **FD** possesses a high degree of oleophobicity in addition to hydrophobicity.

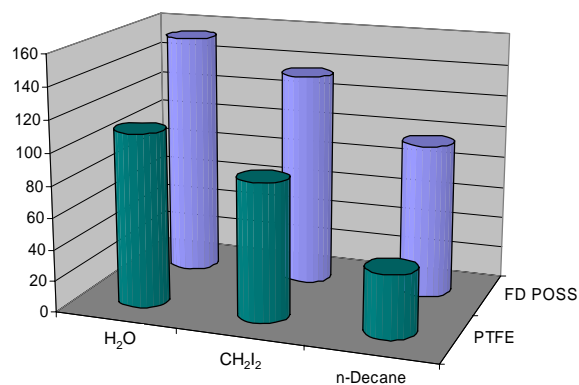


**Figure 4.** Graph comparing **FD** contact angles of water, methylene iodide, and *n*-decane to those of PTFE.

In conclusion, new fluorinated nanoparticles, polyhedral oligomeric silsesquioxanes (F-POSS) have been produced. The synthesis of F-POSS is facile and these compounds can be prepared in nearly quantitative yields and hundred gram quantities, eliminating the need for complex processes and patterning to produce ultrahydrophobic surfaces. To our knowledge, **FD** is the most hydrophobic solid material known. We believe a combination of nano- and micro-scale roughness, in combination with the surface tension of the fluorinated alkyl groups, produces this ultrahydrophobicity.

## Experimental Section

All reagents were purchased from Aldrich or Gelest and purified according to established procedures.<sup>[19]</sup> X-ray crystallography data, surface preparation and analysis, and detailed analytical characterization of F-POSS compounds are included in the Supporting Information.

General procedure for the synthesis of F-POSS compounds **FH**, **FO**, and **FD**: To a 1M solution fluoroalkyltriethoxysilane (10 mmol) in absolute ethanol was added KOH (0.03 mmol) dissolved in deionized water (15 mmol) at room temperature. After continuous stirring for 24 h, the white precipitate was filtered and washed repeatedly with absolute ethanol. The solid was collected and redissolved in AK-225 and residual KOH was extracted by washing repeatedly with deionized water. The organic layer was dried with MgSO<sub>4</sub>, filtered, concentrated and dried in vacuum to afford the F-POSS compound as a white solid in nearly quantitative yield.

Synthesis of F-POSS compound **FP**: Using a modified procedure as previously reported by Fukuda<sup>[20]</sup>, hepta(3,3,3-trifluoropropyl)tricycloheptasilsesquioxane trisodium silanolate (3.5 mmol) in THF (0.05 M) is added 3,3,3-trifluoropropyltrichlorosilane (5.25 mmol) at room temperature. Triethylamine (3.5 mmol) is then immediately added drop wise to the solution. After stirring for 3 h, the white precipitated solids were filtered and the filtrate was concentrated under vacuum. The white solid was then suspended in methanol, filtrated, washed repeatedly with methanol, and dried in vacuum to obtain the title compound as a white powder (80%).

**Keywords:** F-POSS • ultrahydrophobicity • surface roughness • nanoparticle • contact angle

- [1] T. Sun, L. Feng, X. Gao, L. Jian, *Acc. Chem. Res.* **2005**, *38*, 644.
- [2] C. Neinhuis, W. Barthlott, *Ann. Bot.* **1997**, *79*, 677.
- [3] W. Barthlott, C. Neinhuis, *Planta* **1997**, *202*, 1.
- [4] a) N. Takeshita, L. A. Paradis, D. Oner, T. J. McCarthy, W. Chen, *Langmuir* **2004**, *20*, 8131; b) J.-Y. Shiu, C.-W. Kuo, P. Chen, C.-Y. Mou, *Chem. Mater.* **2004**, *16*, 561.
- [5] a) G. Crevoisier, P. Fabre, J.-M. Corpart, L. Leibler, *Science* **1999**, *285*, 1246; b) G. Zhang, D. Wang, Z.-Z. Gu, H. Mohwald, *Langmuir* **2005**, *21*, 9143.
- [6] a) K. K. S. Lau, J. Bico, K. B. K. Teo, M. Chhowalla, G. A. J. Amaratunga, W. I. Milne, G. H. McKinley, K. K. Gleason, *Nano Lett.* **2003**, *3*, 1701; b) E. Hosono, S. Fujihara, I. Honma, H. Zhou, *J. Am. Chem. Soc.* **2005**, *127*, 13458.
- [7] a) Y. H. Erbil, L. A. Demirel, Y. Avci, O. Mert, *Science* **2003**, *299*, 1377; b) M. Morra, E. Occhiello, F. Garbassi, *Langmuir* **1989**, *5*, 872.
- [8] a) R. I. Gonzales, S. H. Phillips, G. B. Hoflund, *J. Spacecraft Rockets* **2000**, *37*, 463; b) S. H. Phillips, T. S. Haddad, S. J. Tomczak, *Curr. Opin. Solid State Mater. Sci.* **2004**, *8*, 21; c) Wright ref
- [9] G. Li, L. Wang, N. Hanli, C. U. Pittman, Jr. *J. Inorg. Organomet. Polym.* **2001**, *11*, 123
- [10] a) T. Koike, M. Takamura, E. Kimura, *J. Am. Chem. Soc.* **1994**, *116*, 8443; b) W. Nam, H. J. Kim, S. H. Kim, R. Y. N. Ho, J. S. Valentine, *Inorg. Chem.* **1996**, *35*, 1045.
- [11] S. I. Troyanov, P. A. Troshin, O. V. Boltalina, I. N. Ioffe, L. N. Sidorov, E. Kemnitz, *Angew. Chem. Int. Ed.* **2001**, *40*, 285.
- [12] A. Herzog, R. P. Callahan, C. L. B. Macdonald, V. M. Lynch, M. F. Hawthorne, R. J. Lagow, *Angew. Chem. Int. Ed.* **2001**, *40*, 2121.
- [13] T. Hayashi, M. Terrones, C. Scheu, Y. A. Kim, M. Rühle, T. Nakajima, M. Endo, *NanoLett.* **2002**, *2*, 491.
- [14] T. Young, *Phil. Trans. Roy. Soc.* **1805**, *95*, 65.
- [15] A. B. D. Cassie, S. Baxter, *Tran. Faraday Soc.* **1944**, *40*, 546.
- [16] R. N. Wenzel, *Ind. Eng. Chem.* **1936**, *28*, 988.
- [17] A. Bondi, *J. Phys. Chem.* **1966**, *70*, 3006.
- [18] a) F. Müller-Plather, S. Pal, H. Weiss, H. Keller, *Soft Mater.* **2005**, *3*, 21; b) P. F. Rios, H. Dodiuk, S. Kenig, S. McCarthy, A. Dotan, *J. Adhesion Sci. Technol.* **2006**, *20*, 563.
- [19] W. L. F. Armarego, D. D. Perrin, *Purification of Laboratory Chemicals*, Boston, Butterworth Heinemann, **1996**.
- [20] K. Koh, S. Sugiyama, T. Morinaga, K. Ohno, Y. Tsujii, T. Fukuda, M. Yamahiro, T. Iijima, H. Oikawa, K. Wantanabe, T. Miyashita, *Macromolecules* **2005**, *38*, 1264.

Received: ((will be filled in by the editorial staff))

Published online on ((will be filled in by the editorial staff))

## Entry for the Table of Contents (Please choose one layout)

Layout 1: 1<sup>st</sup> choice (for cover)

### Ultrahydrophobic Nanospheres

Joseph M. Mabry,\* Ashwani Vij,\* Scott T. Iacono, and Brent D. Viers

Page – Page

Ultrahydrophobic Fluorinated Polyhedral Oligomeric Silsesquioxanes (F-POSS)



Ultrahydrophobic Fluorinated POSS compounds have been easily produced by the base-catalyzed condensation of trifunctional silanes. These compounds exhibit water contact angles up to 154° and are the most hydrophobic and lowest surface tension crystalline solids known. This extreme hydrophobicity can be explained by the degree of fluorination, as well as the combination of nano- and micro-scale surface roughness of the prepared surfaces. These nanoparticles may be useful in a variety of polymer nanocomposites.

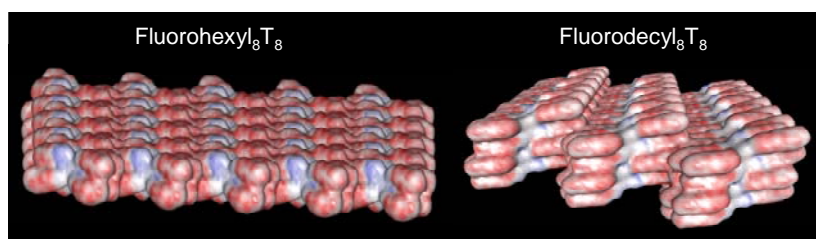
Layout 2: 2<sup>nd</sup> choice

### Ultrahydrophobic Nanospheres

Joseph M. Mabry,\* Ashwani Vij,\* Scott T. Iacono, and Brent D. Viers

Page – Page

Ultrahydrophobic Fluorinated Polyhedral Oligomeric Silsesquioxanes (F-POSS)



Ultrahydrophobic Fluorinated POSS compounds have been easily produced by the base-catalyzed condensation of trifunctional silanes. These compounds exhibit water contact angles up to 154° and are the most hydrophobic and lowest surface tension crystalline solids known. This extreme hydrophobicity can be explained by the degree of fluorination, as well as the combination of nano- and micro-scale surface roughness of the prepared surfaces. These nanoparticles may be useful in a variety of polymer nanocomposites.

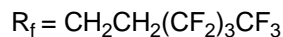
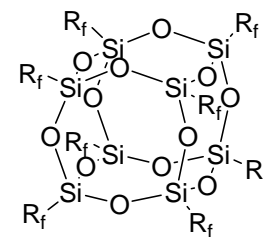
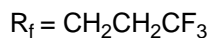
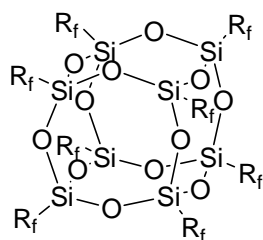
# Ultrahydrophobic Fluorinated Polyhedral Oligomeric Silsesquioxanes (F-POSS)

Joseph M. Mabry,\* Ashwani Vij,\* Scott T. Iacono, and Brent D. Viers  
*Air Force Research Laboratory, Propulsion Directorate,  
Edwards Air Force Base, CA 93524 USA*

## Supporting Information

**Instrumentation.**  $^1\text{H}$ ,  $^{19}\text{F}$ , and  $^{29}\text{Si}$  NMR data was obtained on a Bruker AXS SMART APEX and chemical shifts were reported in part per million ( $\delta$  ppm).  $^1\text{H}$  NMR was reported downfield from tetramethylsilane ( $\delta$  0.0) and are, in all cases, referenced to the residual proton resonance peaks:  $\delta$  7.24 for chloroform-*d* and  $\delta$  2.09 for acetone-*d*<sub>6</sub>.  $^{19}\text{F}$  NMR was referenced to  $\text{CFCl}_3$  and recorded with proton decoupling.  $^{29}\text{Si}$  NMR was referenced to tetramethylsilane ( $\delta$  0.0) and was recorded with inverse-gated proton decoupling with a 12 second pulse delay in order to minimize (negative) nuclear Overhauser effects. Coupling constants for all spectra are reported in Hertz (Hz). Atomic force microscopy (AFM) was conducted on a Nanoscope IV controller (3100 SPM Head) in tapping mode. Etched Silicon probes of nominal spring resonance 300 kHz (spring constant approx. 0.3 mN/m) were used for light tapping (driving amplitude ca 1.1 V) of varying section size at 1–2 Hz collection times (512 points/line).

**Contact Angle Measurements.** Powder surfaces were prepared by dissolving the fluoroalkyl POSS in the minimal amount of AK-225 (Asahi Glass Co.). The surfaces were spin cast (2000 RPM) onto a mica surface (water contact angle  $32^\circ$ ) and produced well-adhered, opaque coatings. Contact angle analysis was performed on a FDS Dataphysics Contact Analyzer System. The contact angles were determined via the software suite. Static water contact angle values reported were an average of three values measured on various areas of the coated surface.

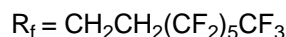
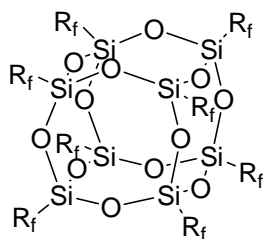


**Analytical Data for 3,3,3-trifluoropropyl<sub>8</sub>T<sub>8</sub> (Fluoropropyl POSS, FP).** Mp 234–237 °C (from THF);  $^1\text{H}$  NMR ( $(\text{CD}_3)_2\text{CO}$ , 300 MHz):  $\delta$  2.35–2.28 (m, 16H), 1.04–0.99 (m, 16H);  $^{29}\text{Si}$  NMR ( $(\text{CD}_3)_2\text{CO}$ , 59.6 MHz):  $\delta$  –67.3;  $^{19}\text{F}$  NMR ( $(\text{CD}_3)_2\text{CO}$ , 376 MHz):  $\delta$  –69.8 (24F); Anal. Calcd for  $\text{C}_{24}\text{H}_{32}\text{F}_{24}\text{O}_{12}\text{Si}_8$ : C, 24.16; H, 2.70; F, 38.21. Found: C, 24.33; H, 2.66; F, 38.45.

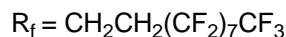
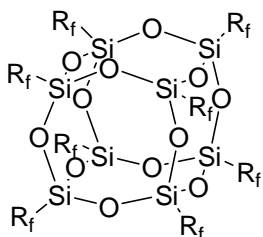
**Analytical Data for 1H,1H,2H,2H-nonafluorooctyl<sub>8</sub>T<sub>8</sub> (Fluorohexyl POSS, FH).** Fluorohexyl POSS (FH) was prepared using perfluorobutylethylenetriethoxysilane as a precursor and is prepared employing the following procedure. Perfluorobutylethylene (donated by DuPont fluoroproducts) (0.25 mol), trichlorosilane (0.30 mol), and  $\text{H}_2\text{PtCl}_6$  (0.025 mol, 2 M in isopropanol) were charged in a sealed tube. The vessel was purged with nitrogen, sealed, and



placed in a preheated oil bath at 80 °C for 24 h. The crude mixture was fractionally distilled to obtain the perfluorobutylethylenetrichlorsilane as a colorless liquid (80%). The pure product is then placed neat in a solution of triethylorthoformate and heated to 110 °C for 48 h. The mixture was fractionally distilled to obtain the perfluorobutylethylenetriethoxysilane as a colorless liquid (70%).  $^1\text{H}$  NMR ( $(\text{CD}_3)_2\text{CO}$ , 300 MHz):  $\delta$  2.34–2.25 (m, 16H), 1.14–1.08 (m, 16H);  $^{29}\text{Si}$  NMR ( $(\text{CD}_3)_2\text{CO}$ , 59.6 MHz):  $\delta$  –66.9;  $^{19}\text{F}$  NMR ( $(\text{CD}_3)_2\text{CO}$ , 376 MHz):  $\delta$  –82.5 (24F), –117.2 (16F), –125.2 (16F), –127.1 (16F).



**Analytical Data for 1H,1H,2H,2H-tridecafluorooctyl<sub>8</sub>T<sub>8</sub> (Fluorooctyl POSS, FO).** Mp 120 °C (from THF);  $^1\text{H}$  NMR ( $(\text{CD}_3)_2\text{CO}$ , 300 MHz):  $\delta$  2.51–2.38 (m, 16H), 1.29–1.25 (m, 16H);  $^{29}\text{Si}$  NMR ( $(\text{CD}_3)_2\text{CO}$ , 59.6 MHz):  $\delta$  –67.0;  $^{19}\text{F}$  NMR ( $(\text{CD}_3)_2\text{CO}$ , 376 MHz):  $\delta$  –83.4 (24F), –118.3 (16F), –123.6 (16F), –124.6 (16F), –125.0 (16F), –128.1 (16F); Anal. Calcd for  $\text{C}_{24}\text{H}_{32}\text{F}_{24}\text{O}_{12}\text{Si}_8$ : C, 24.07; H, 1.01; F, 61.87. Found: C, 24.26; H, 0.96; F, 62.07.



**Analytical Data for 1H,1H,2H,2H-heptadecafluorodecyl<sub>8</sub>T<sub>8</sub> (Fluorodecyl POSS, FD).** Mp 150 °C (from THF);  $^1\text{H}$  NMR ( $(\text{CD}_3)_2\text{CO}$ , 300 MHz):  $\delta$  2.49–2.36 (m, 16H), 1.26–1.22 (m, 16H);  $^{29}\text{Si}$  NMR ( $(\text{CD}_3)_2\text{CO}$ , 59.6 MHz):  $\delta$  –67.0;  $^{19}\text{F}$  NMR ( $(\text{CD}_3)_2\text{CO}$ , 376 MHz):  $\delta$  –83.3 (24F), –118.1 (16F), –123.5 (48F), –124.3 (16F), –125.0 (16F), –128.0 (16F); Anal. Calcd for  $\text{C}_{24}\text{H}_{32}\text{F}_{24}\text{O}_{12}\text{Si}_8$ : C, 24.06; H, 0.81; F, 64.70. Found: C, 24.32; H, 0.82; F, 64.82.

**X-Ray Structures for Fluorinated POSS Compounds.** Crystallographic data for **FP**, **FH**, **FO**, and **FD** have been submitted to the Cambridge Crystallographic Data Center with publication numbers CCDC 629369, 608207, 608208, and 607209, respectively. Copies can be obtained free of charge from CCDC, 12 Union Road, Cambridge, CB2 1EZ, UK (e-mail: deposit@ccdc.cam.ac.uk).



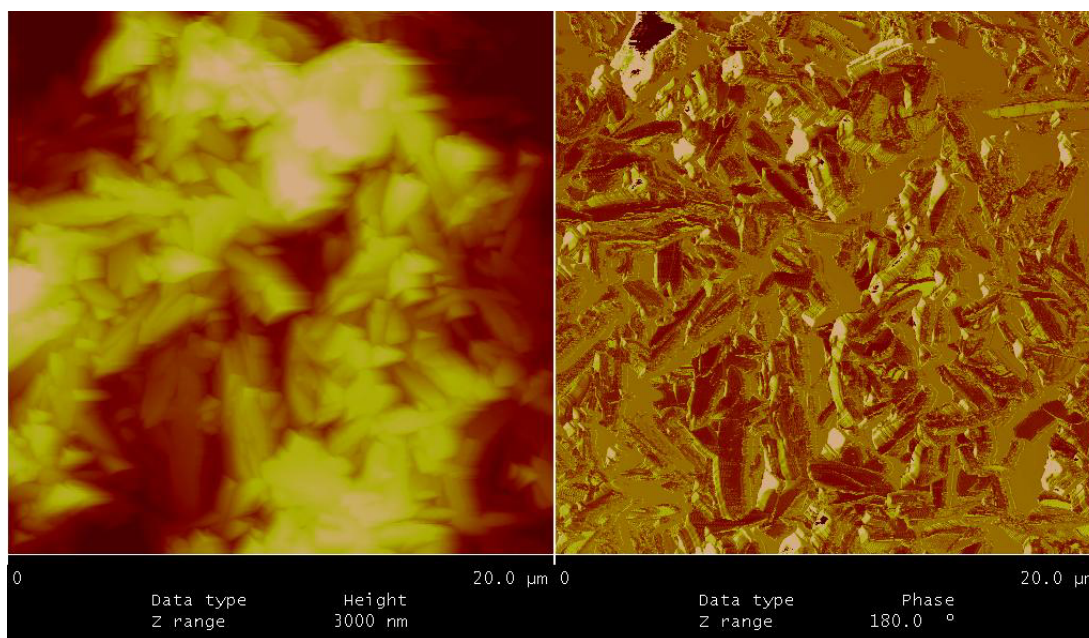


**Figure 1.** AFM analysis of the height (left inset) and phase (right inset) image of spin cast film surface of **FD**.

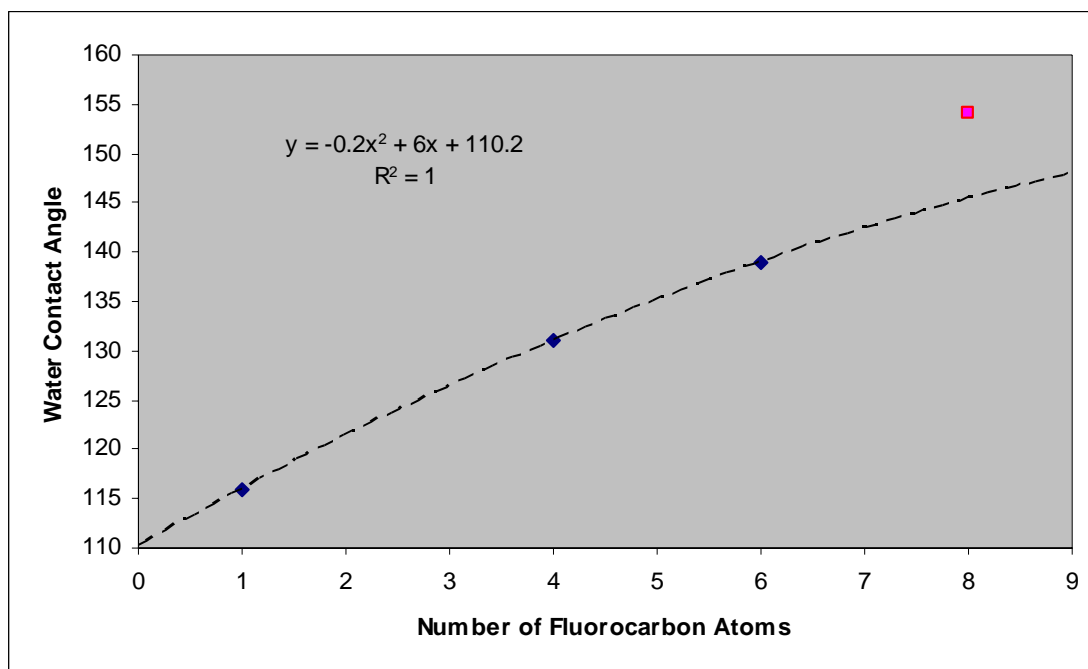


**Figure 2.** Nanoroughness of **FD** contributes to the increase in the observed water contact angle compared to the theoretical prediction. The theoretical water contact angle is determined by plotting water contact angle versus fluorocarbon chain length, as observed in many systems. Based on the regression analysis of various fluorocarbon chain lengths, **FD** has a theoretical water contact angle of 145°. The observed **FD** water contact angle (154°) is 9° higher than the theoretically determined value.



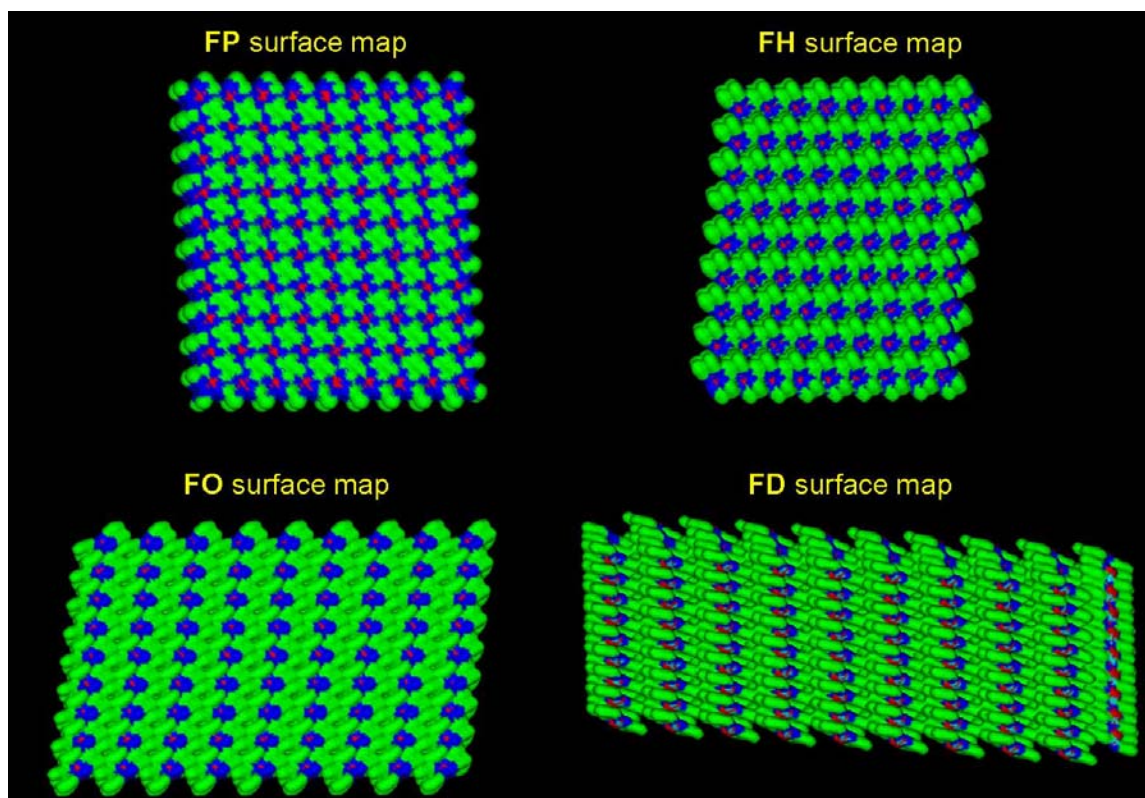


**Figure 5.** Surface element maps of **FP**, **FH**, **FO**, and **FD** surfaces, respectively. Fluorine is shown in green, hydrogen is shown in blue, and the POSS cage is shown in red.

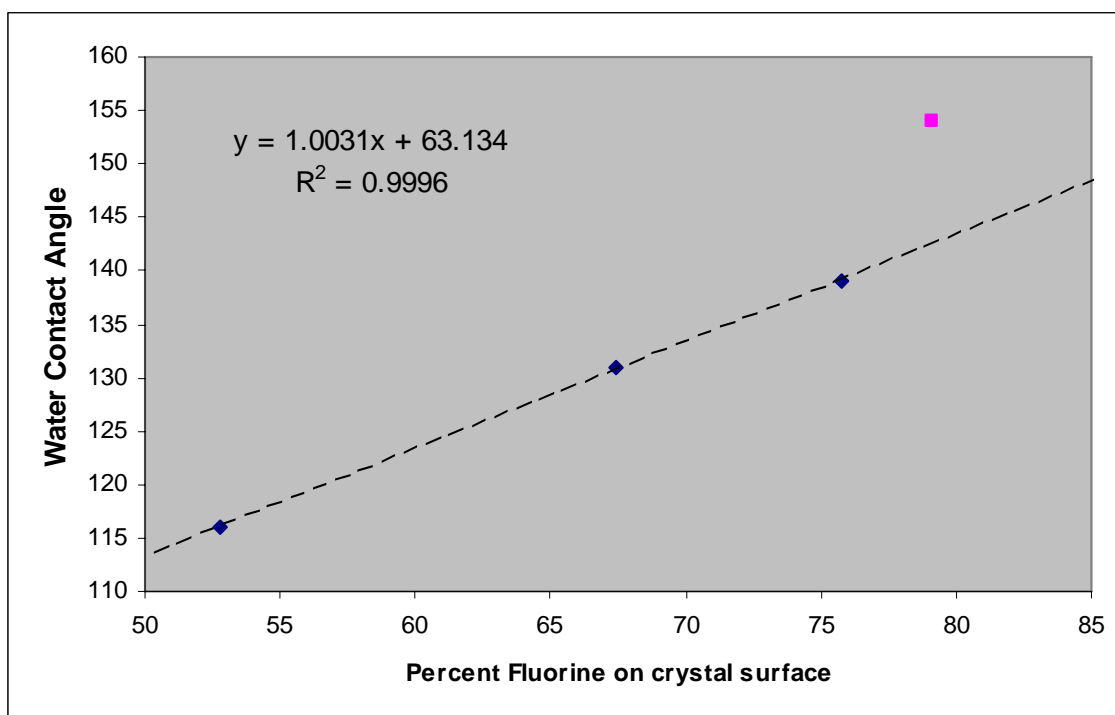
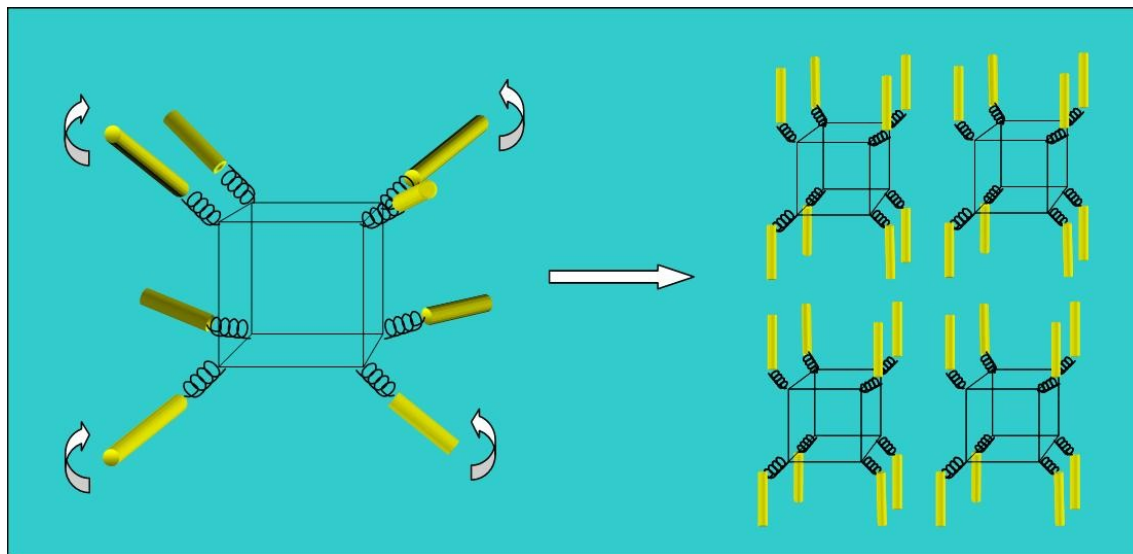


**Figure 6.** Plot of percent fluorine vs. contact angles for F-POSS compounds. The expected **FD** contact angle is 142°, while the actual contact angle is 154°, 12° higher than the theoretical value.

The ability to crystallize F-POSS from fluorinated solvents, using solvent evaporation/vapor diffusion techniques, enabled the growth of single crystals for high resolution (0.75 Å) x-ray diffraction studies. At room temperature, a diffused diffraction pattern indicates immense disorder with the crystal lattice due to high entropy of the fluorinated alkyl chains. Our initial attempts to cool these crystals to 100K resulted in disastrous loss of sample from the goniometer head with crystals literally “exploding”. Our relentless efforts, and repeated cell determinations at ten-degree intervals starting at 273K, later proved that these “explosions” for **FO** and **FD** occur due to a crystal phase transition (with doubling of the *b*-axis) between 213 and 198K. Once we were able to slowly pass this phase transition, the crystals could be rapidly cooled to 100K. At this temperature, the diffraction spots became intense, well defined and lost majority of the low-angled diffused scattering pattern.

With the exception of **FP**, which is tetragonal (*I*-4), the remaining compounds are triclinic (*P*-1). In the case of **FH** and **FD**, the asymmetric unit contains one and two crystallographically independent “half” molecules, respectively. In both cases, there is an inversion center in the middle of the POSS core, which results in 4 pairs of fluoroalkyl with similar conformation. The structure of **FO** lacks this inversion symmetry and, therefore, contains eight independent fluoroalkyl chains with varying conformations.

The molecular structure of F-POSS contains rigid, rod-like fluoroalkyl chains which are attached to the silicon atoms of rigid POSS cage via flexible, spring-like -CH<sub>2</sub>CH<sub>2</sub>- (hydrocarbon) chain. The relative arrangement of these components and resulting molecular interaction determines their surface properties and, therefore, the scale of hydrophobicity for F-POSS materials. For example, the crystal structure of **FP** shows that the fluoroalkyl chains radiate diagonally from the corners of the POSS cage, which is different from the other F-POSS structures, which show a near-parallel arrangement of these fluoroalkyl chains (Figure 4). This difference can be attributed to the formation of strong intramolecular interactions between strongly electropositive Si and electron rich fluorine atoms in **FH**, **FO**, and **FD**, which act as molecular “anchors.” These intramolecular contacts of ~3.0 Å are significantly shorter than the sum of van der Waal radii for silicon and fluorine at 2.10 and 1.47 Å, respectively.<sup>[17]</sup> Consequently, these interactions act as molecular “anchors” which ties down the chains close to the POSS cage, thereby exposing it for strong intermolecular Si...F contacts (~3.5 Å) for lattice construction.



It is interesting to note that **FP** lacks any intramolecular Si...F contact but shows four pairs of identical (symmetry imposed) Si...F contacts at 3.479 Å, which originate from four of eight fluoropropyl chains causing the POSS cages to stack up along the *c*-axis.

In **FH**, the asymmetric unit contains half the molecule with an inversion center generating the other half of the molecule. The fluoroethyl chains located on Si1, Si2 and Si4 are in a staggered conformation whereas the fourth fluoroethyl chain on Si3 is twisted in a quasi “boat” conformation. The latter conformation results in a strong intramolecular Si...F contact at 3.089 Å, thereby restricting the “floppiness” of this fluoroethyl chain. The crystal lattice is built by two symmetry generated weak Si...F intermolecular contacts between Si1 and F33 atoms (~3.51 Å), resulting in a parallel stacking of molecules. The network is then extended in the third dimension via formation of H...F interactions of 2.489 Å along the *a*-axis. The terminal fluorine atoms of fluoroethyl chains located on Si2 and Si4 hydrogen bond to a hydrogen atom on both alpha- and beta-carbons on Si3 around 2.63 Å, which is on the borderline of sum of van der Waal distance of Si and F at 2.67 Å. For the remaining **FO** and **FD** structures, **FO** shows molecules lacking any internal symmetry whereas for **FD**, there are two crystallographically independent “half” molecules in the asymmetric unit with an inversion symmetry lying in the center of the POSS core. In the case of **FO**, out of eight total fluorocarbon chains, only two (located on Si1 and Si8) adopt an exclusive chair conformation, where the remaining six chains have both chair and boat conformation giving rise to intramolecular as well as intermolecular Si...F bonding. The intramolecular contacts between Si3 and Si5 with fluorine atom located on a  $\gamma$ -carbon atoms is relatively strong at ~3.15 Å, which anchors the fluoroalkyl chains to the core. Fluorine atoms bonded to fifth and sixth carbon atoms on the neighboring Si6 straddle across an adjacent POSS cage resulting in the formation of intermolecular Si...F contacts, with distances of 3.521 and 3.507 Å, respectively, along the [0 1 1] plane. The crystal packing shows almost parallel stacking of the molecules with the POSS core almost collinear with the fluoroalkyl chains (mean least square plane between POSS cage and fluoroalkyl chains in chair conformation = ~80°). Contrary to these observations, the packing of **FD** shows the POSS cores twisted with respect to the fluoroalkyl chains (mean least square plane between POSS cage and fluoroalkyl chains in chair conformation = ~104°), resulting in a zig-zag packing as opposed to a co-linear packing in **FO**. It is important to point out that this difference stems from the intermolecular interactions that result from fluorine atoms located on third and fourth carbon atoms with Si5 and Si8 of the neighboring POSS cage, which in turn mirrors this bonding behavior yielding a dimeric structure. This dimeric structure is further expanded by Si...F interactions from above and below the exposed POSS cage.

Bullets for cover letter:

- Ultrahydrophobic nanoparticles
- Nanoroughness improves hydrophobicity
- Correlation of single crystal X-ray structures and hydrophobicity
- Most hydrophobic crystalline solid known